Quantum Mechanical Study of the Correlation of Attack and Recoil Angles for the Cl + H_2 Reaction Using the Stereodirected and Discrete Variable Representations on Two Potential Energy Surfaces†

Dimitris Skouteris* and Antonio Laganà

Dipartimento di Chimica, Università di Perugia, Perugia 06123, Italy

Received: August 4, 2005; In Final Form: September 23, 2005

The zero total angular momentum ($J = 0$) S matrix elements, calculated using a time-dependent wave packet method for the Cl (^{2}P) + H_2 reaction on two different potential energy surfaces, have been matrix transformed to the stereodirected and Gauss−Legendre discrete variable representations. Although the results in the two representations are (as expected) quantitatively different with respect to the angular selectivity and specificity of the reactive process, the qualitative similarity has allowed us to draw for the first time conclusions with respect to some characteristics of the potential energy surface.

1. Introduction

The most detailed result of any reaction dynamics calculation (indeed, any scattering calculation) is the S matrix element between a well-specified reactant state (including parameters such as total angular momentum J and its projection) and a well-specified product state. Knowing the S matrix allows full knowledge of the scattering wave functions and hence, according to quantum mechanics, full information about the system under consideration.

An obvious question regards the representation of reactant and product states in which the S matrix should be expressed. Normally, for systems comprising an atom and a diatomic molecule (henceforth referred to as A + BC systems), states are labeled by vibrational (v) and rotational (j) quantum numbers (vj representation). The reason for such a choice is also obvious. In fact, related state to state elements not only give us physical insight into the process (since they are directly related to the corresponding classical momenta) but also, being functions of the energy of the system, can be immediately correlated to the results of experiments with time-of-flight or spectroscopic detection.

However, it is equally obvious that this is not the only choice of representation that one can make. In quasiclassical trajectory calculations (QCT), this is a problem of less relevance because the use of the classical phase space delivers complete information on both coordinates and momenta. On the other hand, the possession of such information in a quantum mechanical context is precluded by the uncertainty principle. Nevertheless, one can resort to the use of representations whose S matrix can conceivably provide complementary information to the standard one, i.e., more coordinate- as opposed to momentum-oriented. Obviously, such information comes at the cost of sacrificing some momentum-related data. The use of these alternative representations can be of help in elucidating the results of stereodynamic experiments.[1,2]

An elegant way of tackling this problem has been worked out by Aquilanti and co-workers[3,4] by exploiting the properties of the stereodirected representation (SDR). The SDR method has been utilized to tackle systems such as Na + HF,[5] Sr + HF,[6] F + HCl,[7] C + CH,[8,9] and F + H_2.[10] Alvariño et al. have used SDR to assess the correlation between attack and recoil angles for the Li + HF reaction.[11,12] Miranda et al.[13] have also followed up on this, using three different methods to explore the same correlation for the Li + HF reaction at a total angular momentum of $J = 0$. The representations used by Miranda were the SDR, as well as the preferred attack angle (PAA) method, where the coherent combinations of spherical harmonics were deliberately chosen either to maximize the squared amplitude around certain angles or to maximize/minimize the total reaction probability.

However, the PAA approach does not lead to a simple analytical formulation of the coefficients ensuring the maximization of the amplitude around a given value of the angle (essentially at each point a matrix inversion would be required). Moreover, maximization of the amplitude at a given point does not necessarily imply a higher degree of localization of the wave function around this point. For this reason, to confront the SDR with an alternative approach, we chose to resort to the use of the Gauss−Legendre discrete variable representation (DVR), originally developed by Light and co-workers.[14−16] It is, in fact, well-known that DVR wave functions exhibit a high degree of localization around the Gauss−Legendre quadrature points and would thus seem ideal for our purpose.

In the present paper, the comparison is performed for the Cl + H_2 reaction at zero total angular momentum ($J = 0$)[17,18] using the S matrix elements obtained from a time-dependent wave packet calculation. This reaction has received a lot of attention in recent years from both a theoretical and an experimental point of view.[19−23] The calculations were performed using two different potential energy surfaces (PESs) having different angular anisotropies. One is the semiempirical surface (G3) introduced in 1996 by Allison et al.,[24] and the other is the ground component of the surfaces calculated recently by Capecchi and Werner.[25,26] This latter one is based on the older BW surface,[27] differing in the rigorous treatment in it of the spin−orbit coupling.

The S matrix is then transformed into the SDR and the DVR representations, which essentially constitute linear combinations

† Part of the special issue "John C. Light Festschrift".

* To whom correspondence should be addressed. Tel: 0039-075-5855513. Fax: 0039-075-5855606. E-mail dimitris@dyn.unipg.it.

10.1021/jp054330n CCC: $33.50
Published on Web 11/01/2005

of reactant and product rotational states. We subsequently calculate reaction probabilities in these alternative representations to work out information regarding the angular dependence of the reaction and, in particular, the correlation between the attack and the recoil angles of the triatomic system.

The organization of this paper is as follows: in section 2, the computational procedure is explained, along with the two angle specific representations utilized. In section 3, results are presented and a discussion is made in order to connect the observed trends with the key features of the PESs involved. In section 4, some conclusions are given.

2. Computational Procedure

2.1. S Matrix Transformation. As has been described in detail elsewhere,[17,18] the S matrix elements are obtained from RWAVEPR, a standard wave packet calculation program, which propagates an initial state-selected wave packet in product Jacobi coordinates so as to achieve full product state resolution. In this calculation, all S matrix elements refer to a total angular momentum of $J = 0$ (excluding the electronic angular momentum).

The propagation does not take place in real time but, rather, in the discrete index of the expansion of the outgoing Green's function in terms of Chebyshev polynomials of an appropriately scaled Hamiltonian. The S matrix element from a channel av to a channel cv' is subsequently derived from the relation

$$S_{cv',av} \propto \frac{\langle w_p \,|G^+(E)|\, w_r\rangle}{\langle w_p \mid cv'\rangle \langle av \mid w_r\rangle} \tag{1}$$

where w_p and w_r are wave packets localized in the product and reactant regions, respectively. With this method, one cannot actually follow the evolution of the system wave packet during the reactive event as it is propagating. However, this is an unimportant loss of information as the quantity of interest is the S matrix. As a matter of fact, the method retains the well-known advantage of time-dependent methods (namely, that of obtaining the S matrix elements for many energies with only one calculation), and the use of eq 1 makes it easier to deal with all values of J. Unfortunately, one still has to execute one calculation for each different initial state of the reactants.

Once the S matrix is obtained in this way, it is expressed in what was termed before the vj representation. This can be transformed to an alternative representation using the standard technique of matrix transformation by inserting two complete sets into the matrix element of the $\hat{S}$ operator:

$$\langle v't' \mid \hat{S} \mid vt\rangle = \sum_{jj'} \langle v't' \mid v'j'\rangle \langle v'j' \mid \hat{S} \mid vj\rangle \langle vj \mid vt\rangle \tag{2}$$

Here, t denotes a generic quantum number. However, to derive information relevant to establishing correlations between attack and recoil angles, the vt wave functions should be localized as much as possible around a restricted interval of angle values. This way, the transformed S matrix elements provide us with information regarding angular selectivity and specificity of the reaction under consideration. The angles mentioned here are termed as attack and recoil angles for the reactant and product arrangements, respectively. The attack angle θ_a is defined (for a generic A + BC system) as the angle formed by the interatomic vector of the reactant diatom (the BC vector) and the vector pointing from the center of mass of the diatom toward the atom (the A − BC vector) as shown in the left-hand side scheme of Figure 1. The recoil angle θ_r is

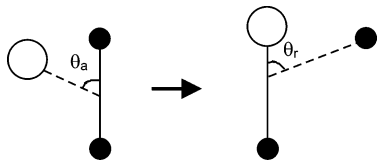

Figure 1. Illustration of a three-particle collision, along with the definition of attack and recoil angles as used in the text.

defined as the angle formed by the interatomic vector of the product diatom and the vector pointing from the center of mass of the product diatom toward the atom (see right-hand side scheme of Figure 1). Being essentially altitude angles, both θ_a and θ_r range between 0 and 180°. Obviously, the vt representation is discrete in the same way that the vj representation is, and some degree of angular delocalization is always to be expected.

The uncertainty principle between angle and angular momentum is a limit to the angular resolution that can be obtained. The more the angle is to be localized, the larger is the number of j states that have to be included in the set. Conversely, the fewer j states are included, the more diffuse the angle-localized wave function is going to be. In our angle-localized basis set, the maximum j (j_{max}) that we are using must be included as an extra parameter, as the resulting angle-localized wave function will certainly depend on its value.

Another limit is imposed by energy conservation. If the total energy of our reactant or product state is known and fixed, the number of diatomic j states that we can coherently combine is obviously bounded up by energetic considerations. Hence, other things (such as moments of inertia of the relevant diatomic molecule) being equal, low total energy necessarily implies a low angular resolution.

There is one more complication that should be considered. Because the angle-localized wave functions result from the coherent superposition of wave functions with a definite j and total energy, this implies that the translational part of the wave function will be different for each j state. In other words, written more fully, an angle specific wave function at a fixed total energy will have the form:

$$|\, t\,\rangle = \sum_j c_j \;|j\,\rangle\, e^{-ikR} \tag{3}$$

$$k^2 = 2\mu(E_{tot} - E_j) \tag{4}$$

where R is the intermolecular separation and c_j values are coefficients determined by us. From the j dependence of k, it is obvious that each j state will be included in the sum with its own phase factor, which will depend on R. If, instead, one attempts to use a fixed translational as opposed to total energy, each j state will correspond to a different total energy, and what is now a phase dependence on distance, will then be a phase dependence on time because of the time-dependent phase factor involving the total energy. Either way, the angular orientation of our wave function is not permanent, as a result of its spatial or temporal distortion. Given the fact that normally, in experiments, the relative translational energy of the reagents is independent of the way that they have been prepared as regards their mutual orientation/alignment, the second method probably provides a more "physical" picture of an actual process. However, it is reminded that, ideally, we are considering processes where the uncertainty in the energy caused by the superposition of rotational states is relatively small (where this is possible). As a result, the use of a fixed total or translational

energy will not have a large effect on the results and the advantages of a fixed total energy (in particular, the possibility of a simple S matrix transformation) can be exploited.

Because of the considerations above, the angle around which our wave function is localized is only valid near $R = 0$, i.e., when the atom is at the center of mass of the diatomic and all phase factors e^{-ikR} are equal to 1. Thus, the terms attack angle and recoil angle are understood to mean the angles as defined before, but the wave functions themselves strictly refer to the hypothetical angles when the atom would be very close to the center of mass of the diatomic (in either the reactant or the product arrangements) in the absence of any intermolecular potential.

Obviously, the point $R = 0$ is impossible to reach for a reaction such as $Cl + H_2$, which is dominated by a repulsive surface. However, the R range over which the wave function remains more or less intact can be estimated by uncertainty principle arguments. In particular, it is given by

$$\delta R = \left(\frac{2E_t}{\mu}\right)^{1/2} \frac{\pi}{\delta E} \tag{5}$$

where δR is the range of R, E_t and δE are the translational energy and its spread as a result of superposition, respectively, and μ is the reduced mass of the approaching units. Substituting typical values of $E_t = 0.3$ eV, $\delta E = 0.05$ eV, and $\mu = 1.0$ amu for the $H + HCl$ arrangement, one obtains a δR of the order of 6 bohr, which is well beyond the transition state and the product van der Waals well for the reaction. Thus, the effects of the transition state and long range dynamics on the products are expected to be reliably reflected on our transformed S matrix. In the case of the reactant $Cl + H_2$ arrangement, as a result of the increased range of energies mixed and the larger reduced mass, δR is smaller (around 3 bohr). Thus, long range effects on the reagent angular distribution (as is the case in the CW surface) are possibly subject to this uncertainty principle effect. Each possible representation is essentially defined by its set of matrix elements $\langle t \mid j \rangle$ as shown in eq 2, where $\mid j \rangle$ is a ket in the j representation and $\mid t \rangle$ is a ket in the angle-localized representation. What follows is a short description of each of the two representations used in the present work.

2.2. SDR. As already mentioned, the SDR representation has been developed by Aquilanti and co-workers.[3,4] The matrix elements connecting it with the j representation are given by the equation:

$$\langle j \mid t \rangle = (-1)^{j-t+j_{max}/2} \left\langle \frac{j_{max}}{2} t, \frac{j_{max}}{2} - t \,\middle|\, j0 \right\rangle \tag{6}$$

where the bracket implies a Clebsch−Gordan coefficient. From these notations, we see that the relevant t quantum number takes values

$$t = \frac{j_{max}}{2}, \frac{j_{max}-1}{2}, ..., -\frac{j_{max}}{2} \tag{7}$$

The values of t are integrals or half-integrals, depending on whether j_{max} is even or odd, respectively.

The characteristic of the SDR, which is of interest for our purposes, is that as j_{max} tends to infinity, SDR wave functions tend to become localized around a specific angle value obeying the equation:

$$\cos\theta_t^{SDR} = -\frac{2t}{j_{max}+1} \tag{8}$$

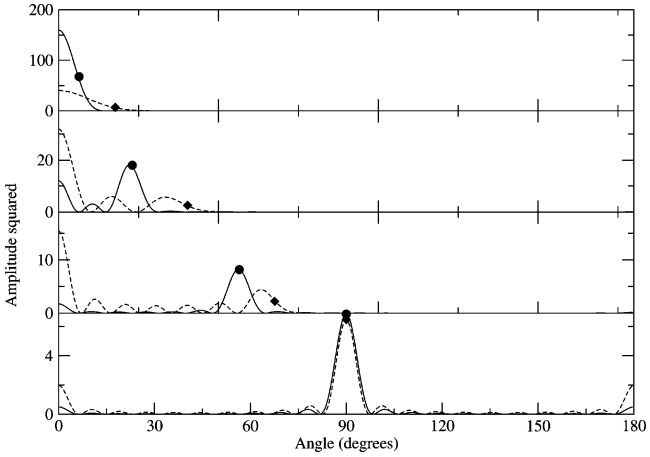

Figure 2. Probability amplitudes plotted as a function of the attack angle for two wave functions in the DVR (solid line) and the SDR representation (dashed line). Here, the maximum j used is 20 in both cases. The heavy points show the related nominal angles.

The angle value given by this formula, θ_t, provides what is going to be termed henceforth the nominal angle for the SDR representation. However, it should be kept in mind that for relatively small j_{max} (as would be, for example, the case for light molecules such as H_2), the angle localization of the SDR wave function becomes poorer, especially for near-collinear configurations.[13]

2.3. Gauss−Legendre DVR. This is the standard angular DVR representation, where the interval between 0 and 180° is discretised by the normal Gauss−Legendre quadrature. This representation was originally used in the area of reaction dynamics by Light and co-workers.[14−16] The relevant matrix element is

$$\langle j \mid t \rangle = w_t^{1/2} P_j(x_t) \tag{9}$$

where x_t is a point in the Gauss−Legendre quadrature, w_t is the corresponding quadrature weight, and P_j denotes a (normalized) Legendre polynomial. Here, t takes integral values between 1 and $j_{max} + 1$. The nominal angle for a wave function in the DVR representation is given by the formula

$$\cos\theta_t^{DVR} = x_t \tag{10}$$

As is also the case for the SDR representation, DVR wave functions tend to localize around their nominal angle as j_{max} tends to infinity and to lose their localization at small j_{max}. However, their advantage over SDR wave functions is that they always retain their global maximum at their nominal angle (given by the Gauss−Legendre quadrature point) and hence are expected to be more "faithful" to the angle that they represent, especially toward collinear configurations and at low j_{max} values. To give an idea, Figure 2 shows probability amplitudes for SDR and DVR wave functions as a function of the attack or recoil angle θ. In both cases, the corresponding nominal angle is also indicated in the figure as a solid point. One can see that, as the angle approaches 0 or 180°, the DVR representation is generally more localized around its nominal angle than the SDR one.

3. Correlation Effects

3.1. Calculations. The two surfaces used for the calculations (the ground component of the ab initio Capecchi−Werner electronic state manifold CW,[25] and the semiempirical G3 surface) have similar barrier and endothermicity features. Yet,

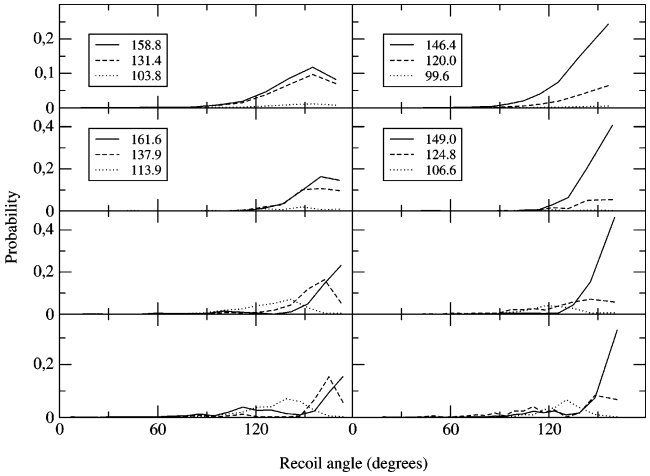

Figure 3. Reaction probabilities plotted as a function of the nominal recoil angle for the G3 surface. The left panels are in the DVR representation, while the right ones are in the SDR one. The total energy increases from 0.5 eV at the top to 0.8 eV at the bottom. The legends show the nominal attack angles in each case.

they differ in the key feature of the dependence of the shape of the interaction on the collision angle. The G3 PES has, in fact, a minimum at collinear configurations (both in the reactant and in the product valley) and a maximum at perpendicular (T-shaped) configurations. On the other hand, the CW PES has an angular local minimum at T-shaped configurations and a maximum at collinear ones (in both reactant and product valleys). The effect is most visible at the van der Waals well, which presents a local minimum with respect to all coordinates (angle and distances) and is found at a T-shaped configuration.

This difference in the anisotropy would be expected to play a significant role in the correlation between attack and recoil angles. Such an effect has already been seen in QCT calculations by Aoiz and co-workers.[20] Our purpose here is to ascertain whether such an effect persists in a quantum mechanical treatment. For this reason, the calculations have been performed at various values of the total energy (namely, 0.5, 0.6, 0.7, and 0.8 eV).

We remind the readers here that the two hydrogen atoms are treated as distinguishable in this calculation. In other words, the reaction that we are studying is $Cl + H_a - H_b$ going to $H_a - Cl + H_b$ where H_a and H_b are distinguishable atoms. From now on, we shall refer to the H atom that eventually forms the HCl molecule as H_a and to the other one as H_b.

3.2. Comparison between the Surfaces and the Representations. The results pertaining to the G3 PES are shown in Figures 3 and 4. The horizontal axis denotes the nominal recoil angle (in degrees), and the vertical axis denotes the corresponding reaction probability. The panels on the left denote the probabilities in the DVR representation, while those on the right are the corresponding ones in the SDR representation. Moreover, the total energy decreases from 0.8 to 0.5 eV in going from the bottom to the top panels.

Two figures are shown, corresponding to two different angular ranges. The first one includes curves from the three attack angles closest to collinear from the H_a atom, while the second one includes the remaining four (three in the case of 0.5 eV, because conservation of energy forbids the inclusion of more states), starting from (almost) perpendicular and going up to collinear from the H_b atom. Hence, the attack angles that are shown for the energy of 0.6 eV are also those for 0.7 and 0.8 eV and are only shown on one panel to avoid congestion. We believe that such an arrangement serves to illustrate the important points to be made about the results.

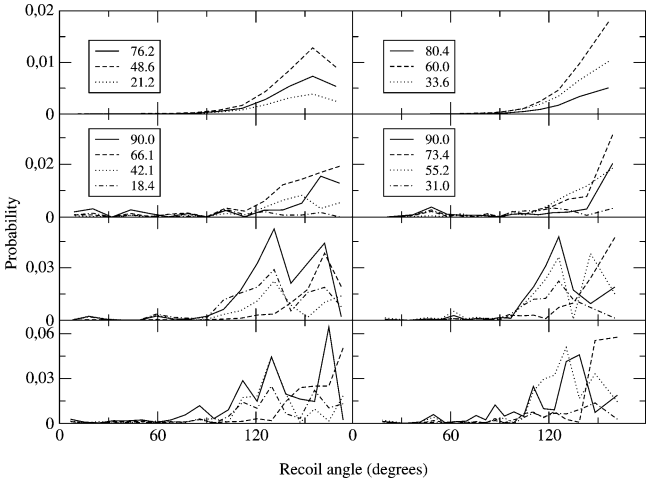

Figure 4. Same as Figure 3 but for nominal attack angles close to the H_b atom.

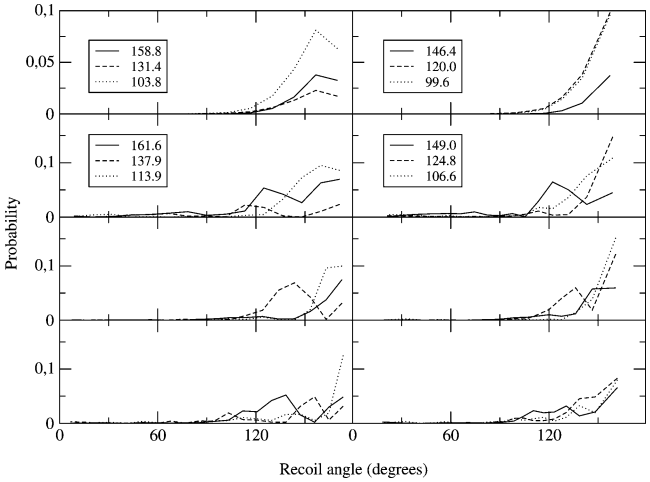

Figure 5. Same as Figure 3 but for the CW surface.

The readers are reminded that the nominal angle can sometimes deviate significantly from the angular region where the corresponding wave function has maximum amplitude. Nevertheless, a clear idea can be formed. All curves are concentrated around the region of 180°. Taking into account the way that the angles are defined in the wave packet program for each particular arrangement, this region corresponds to a collinear $Cl - H - H$ configuration, where the H atom closest to Cl is actually the one with which it is supposed to react, i.e., H_a. Hence, the recoil angle distribution of the probabilities is around the $Cl - H_a - H_b$ arrangement. This corresponds nicely with what is known about the collinear nature of the transition state for both the CW and the G3 surfaces.

Qualitatively, for all four total energies, the curves pertaining to the DVR and the SDR representations are similar. One should always bear in mind the fact that not only are the nominal angles for the two representations different but also the probability distributions are also very different. As a rule, the SDR wave functions are more delocalized, and this effect becomes increasingly apparent near collinear configurations. Turning attention to the reaction selectivity with respect to attack angles, one notices considerable variation between the two surfaces. The corresponding figures regarding the CW surface are Figures 5 and 6. As far as G3 is concerned, reactivity is almost confined to attack angles around 180°, with the angular range widening with increasing collision energy. It can be seen that reactivity drops by almost a factor of 10 between the two collinear ends

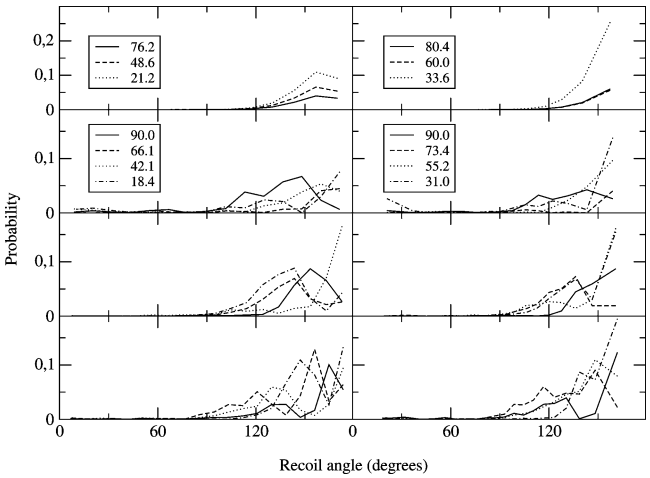

Figure 6. Same as Figure 4 but for the CW surface.

of the spectrum. Our definition of the angles is such that 180° corresponds to a collinear approach from the side of the H_a atom. This behavior can be explained bearing in mind the angular topology of the G3 surface, which aligns the reactants in a collinear configuration before reaction; otherwise, they are simply elastically or inelastically scattered. Moreover, the broadening of the reactive attack angle range with increasing energy can be simply rationalized as an opening up of the cone of acceptance for reaction as the collision energy becomes higher.

Interestingly, while in the DVR representation the reactivity is shared by two or more attack angles (as exemplified by the lowest energy, 0.5 eV), in the SDR representation, the attack angle most toward 180° predominates. This cannot be simply an effect of the SDR wave functions spanning a broader angular range (although of course this factor partially contributes) but is an effect of the phase variation of the wave functions with the angle. In other words, information complementary to the angular one is contained in this curve. It is our belief that this is an example of the selectivity of the G3 surface for low rotational quantum numbers *j*. A very different picture is seen in the case of the CW surface. The recoil angle specificity is, as before, concentrated around 180°, indicating a preference for collinear exit of the reaction products. However, there is no consistency in terms of selectivity with respect to the attack angle. Reactivity appears to be of the same order for all attack angles, and any selectivity seems to be local. For example, at the lowest energy (0.5 eV), reactivity is marginally maximal for near-perpendicular attacks, as well as attacks from the H_b atom. In general, near-collinear attacks from the H_a atom do not seem to promote a reaction as they do in the case of the G3 surface and, instead, near-collinear attacks on the H_b atom are nearly as effective.

Such an effect can be rationalized in terms of the topology of the CW surface, which tends to divert the incoming reactant system toward a perpendicular (T-shaped) configuration and thus away from the transition state. As a result, the incoming geometry is much less crucial in the promotion of reactivity. According to this point of view, reactivity would be much more susceptible to subtle topological effects once the system finds itself at the transition state.

An interesting effect seen at the lowest energy (0.5 eV) for both surfaces, which corroborates what has been said before about the behavior at this low energy, is the fact that all curves have the same form, differing effectively only by a constant factor. This is true for both DVR and SDR representations. Such an effect is suggestive of some kind of memory loss during the reaction event, whereby the difference in attack angle would affect only the overall reactivity but not the recoil angle pattern. This being the lowest collision energy used in the calculations, one can surmise that, classically, the system is moving slowly along the reaction coordinate when it is already on top of the transition state. Thus, it has time to reorient itself while exiting along the product valley in a way independent from the attack angle. On the other hand, at higher energies, the system is moving rapidly in the transition state toward the products and thus has no time for reorientation. In fact, at all other energies, the curves are heavily dependent on the attack angle.

4. Conclusions

The S matrix elements resulting from a quantum mechanical calculation on the $Cl + H_2$ reaction on two different PESs, with different topological characteristics, have been used to investigate the reaction selectivity with respect to various values of the attack angle specificity with respect to product recoil angles, and correlation between the two.

Our findings confirm the conclusions reached using a QCT approach by Aoiz and co-workers.[20] For both surfaces, the recoil angles show maximum probability near 180°, indicating that the predominant arrangement when the system descends toward the product valley is the collinear Cl − H − H one, with the exiting H atom pointing away from the Cl atom. This is in accord with the collinear nature of the transition state, both for the CW and for the G3 surface.

On the other hand, the picture is very different as far as the attack angle is concerned. In the case of the G3 surface, it is seen that only near-collinear attack arrangements on the side of the H_a atom lead to reaction. As the collision energy increases, the range of attack angles that can lead to reaction broadens, and this indicates the opening of the cone of acceptance. Regarding the CW surface, there does not appear to be any preference for a particular attack angle and, at low collision energies, substantial reactivity is seen for a near-collinear approach of the Cl atom toward the H_b atom.

These trends are reminiscent of the conclusions reached by the quasiclassical studies. The topology of the G3 surface directs the incoming Cl atom toward collinear arrangement, thus inducing a strong correlation between reactivity and collinearity. Conversely, the CW topology is such as to direct the Cl atom toward T-shaped arrangements because of the attraction toward the van der Waals well. It appears to be, at least partly, this directing effect which can lead to reaction even if the system approaches the transition state with the wrong collinear orientation.

Acknowledgment. Financial support from ASI, FISR MIUR, and the University of Perugia is acknowledged.

References and Notes

(1) Orr-Ewing, A. J. *J. Chem. Soc. Faraday Trans.* **1996**, *92*, 881.

(2) Loesch, H. J. *Annu. Rev. Phys. Chem.* **1995**, *46*, 555.

(3) Aquilanti, V.; Cavalli, S.; Grossi, G.; Anderson, R. W. *J. Phys. Chem.* **1991**, *95*, 8184.

(4) Anderson, R. W.; Aquilanti, V.; Cavalli, S.; Grossi, G. *J. Phys. Chem.* **1993**, *97*, 2443.

(5) de Miranda, M. P.; Gargano, R. *Chem. Phys. Lett.* **1999**, *309*, 257.

(6) Zhang, L.; Han, K.-L.; Tang, B.-Y.; Yang, B.-H.; Zhang, J. Z. H. *Chem. Phys. Lett.* **2000**, *327*, 381.

(7) Han, K.-L.; Zhang, R.-Q.; Tang, B.-Y.; Yang, B.-H.; Zhang, J. Z. H. *J. Chem. Phys.* **2000**, *113*, 10105.

(8) Han, K.-L.; Tang, B.-Y.; Chen, M.-D.; Zhang, J. Z. H. *J. Chem. Phys.* **2001**, *115*, 731.

(9) Han, K.-L.; Tang, B.-Y.; Chen, M.-D.; Zhang, J. Z. H. *J. Phys. Chem. A* **2001**, *105*, 8629.

(10) Aldegunde, J.; Alvariño, J. M.; de Fazio, D.; Cavalli, S.; Grossi, G.; Aquilanti, V. *Chem. Phys.* **2004**, *301*, 251.

(11) Alvariño, J. M.; Aquilanti, V.; Cavalli, S.; Crocchianti, S.; Laganà, A.; Martinez, T. *J. Chem. Phys.* **1997**, *107*, 3339.

(12) Alvariño, J. M.; Aquilanti, V.; Cavalli, S.; Crocchianti, S.; Laganà, A.; Martinez, T. *J. Phys. Chem.* **1998**, *102*, 9638.

(13) de Miranda, M. P.; Crocchianti, S.; Laganà, A. *J. Phys. Chem. A* **1999**, *103*, 10776.

(14) Lill, J. V.; Parker, G. A.; Light, J. C *Chem. Phys. Lett.* **1982**, *89*, 483.

(15) Light, J. C.; Hamilton, I. P.; Lill, J. V. *J. Chem. Phys.* **1985**, *82*, 1400.

(16) Bacic, Z.; Light, J. C. *Annu. Rev. Phys. Chem.* **1989**, *40*, 469.

(17) Skouteris, D.; Laganà, A.; Capecchi, G.; Werner, H.-J. *Int. J. Quantum Chem.* **2004**, *96*, 562.

(18) Skouteris, D.; Laganà, A.; Capecchi, G.; Werner, H.-J. *Int. J. Quantum Chem.* **2004**, *99*, 577.

(19) Alagia, M.; Balucani, N.; Cartechini, L.; Casavecchia, P.; Van Kleef, E. H.; Volpi, G. G.; Aoiz, F. J.; Bañares, L.; Schwenke, D. W.; Allison, T. C.; Mielke, S. L.; Truhlar, D. G. *Science* **1996**, *273*, 1519. Balucani, N.; Skouteris, D.; Capozza, G.; Segoloni, E.; Casavecchia, P.; Alexander, M. H.; Capecchi, G.; Werner, H.-J. *Phys. Chem. Chem. Phys.* **2004**, *6*, 5007.

(20) Alagia, M.; Balucani, N.; Cartechini, L.; Casavecchia, P.; Volpi, G. G.; Aoiz, F. J.; Bañares, L.; Allison, T. C.; Mielke, S. L.; Truhlar, D. G. *Phys. Chem. Chem. Phys.* **2000**, *2*, 599. Balucani, N.; Cartechini, L.; Casavecchia, P.; Volpi, G. G.; Aoiz, F. J.; Banares, L.; Menendez, M.; Bian, W.; Werner, H.-J. *Chem. Phys. Lett.* **2000**, *328*, 500.

(21) Skouteris, D.; Manolopoulos, D. E.; Bian, W.; Werner, H.-J.; Lai, L. H.; Liu, K. *Science* **1999**, *286*, 1713.

(22) Skouteris, D.; Werner, H.-J.; Aoiz, F. J.; Bañares, L.; Castillo, J. F.; Menendez, M.; Balucani, N.; Cartechini, L.; Casavecchia, P. *J. Chem. Phys.* **2001**, *114*, 10662.

(23) Aoiz, F. J.; Bañares, L.; Castillo, J. F.; Menendez, M.; Skouteris, D.; Werner, H.-J. *J. Chem. Phys.* **2001**, *115*, 2074.

(24) Allison, T. C.; Lynch, G. C.; Truhlar, D. G.; Gordon, M. S. *J. Phys. Chem.* **1996**, *100*, 13575.

(25) Capecchi, G.; Werner, H.-J. *Phys. Chem. Chem. Phys.* **2004**, *6*, 4975.

(26) Alexander, M. H.; Capecchi, G.; Werner, H.-J. *Science* **2002**, *296*, 715.

(27) Bian, W.; Werner, H.-J. *J. Chem. Phys.* **2000**, *112*, 220.